Bulletin of the Seismological Society of America, Vol. 93, No. 6, pp. 2415–2433, December 2003

Inferences Drawn from Two Decades of Alinement Array Measurements of Creep on Faults in the San Francisco Bay Region

by Jon S. Galehouse and James J. Lienkaemper

Abstract We summarize over 20 years of monitoring surface creep on faults of the San Andreas system in the San Francisco Bay region using alinement arrays. The San Andreas fault is fully locked at five sites northwest from San Juan Bautista, the southern end of the 1906 earthquake rupture, that is, no creep (<1 mm/yr) is observed. Likewise, the San Gregorio, Rodgers Creek, and West Napa faults show no creep. The measured creep rate on the Calaveras–Paicines fault from Hollister southward is either 6 or ~10 mm/yr, depending on whether the arrays cross all of the creeping traces. Northward of Hollister, the central Calaveras creep rate reaches 14 ± 2 mm/yr but drops to ~2 mm/yr near Calaveras Reservoir, where slip transfers to the southern Hayward fault at a maximum creep rate of 9 mm/yr at its south end. However, the Hayward fault averages only 4.6 mm/yr over most of its length. The Northern Calaveras fault, now creeping at 3–4 mm/yr, steps right to the Concord fault, which has a similar rate, 2.5–3.5 mm/yr, which is slightly slower than the 4.4 mm/yr rate on its northward continuation, the Green Valley fault. The Maacama fault creeps at 4.4 mm/yr near Ukiah and 6.5 mm/yr in Willits. The central and southern segments of the Calaveras fault are predominantly creeping, whereas the Hayward, Northern Calaveras, and Maacama faults are partly locked and, along with the Rodgers Creek and San Andreas, have high potential for major earthquakes.

Introduction

Having monitored surface creep on strike-slip faults of the greater San Francisco Bay region for more than 20 years, we summarize here our most significant findings regarding temporal and spatial variations in creep rate. We also discuss their possible implications toward a better understanding of the earthquake process and the earthquake hazard posed by these faults. The initial motivation for this project came from a perception that the occurrence of rapid fault creep, relative to earlier in the earthquake cycle, might be immediately precursory to large earthquakes (Allen and Smith, 1966; Brown *et al.*, 1967; Bakun and Lindh, 1985). Although some hope remains that creep-rate anomalies may have predictive value (e.g., Thurber and Sessions, 1998; Bernard, 2001), we now also recognize that long-term creep records may yield more immediate practical benefits by improving our understanding of how spatial and temporal variations in creep rate affect the timing and extent of future earthquake sources and thus can be used to forecast them. We have learned that spatial variation (e.g., variation along strike) in surface creep rate can be used to infer the depth of creeping behavior and thus the extent of locked zones with potential for release in large earthquakes (Savage and Lisowski, 1993; Lienkaemper *et al.*, 2001; Simpson *et al.*, 2001). Temporal variation in creep may result from stress changes induced by moderate and large earthquakes in the region, which may either advance or retard future large earthquakes. (Mavko, 1982; Galehouse, 1997; Lienkaemper *et al.*, 1997; Toda and Stein, 2002).

Fault creep or aseismic slip was first documented on the central San Andreas fault system in 1956 (Steinbrugge and Zacher, 1960). Brown and Wallace (1968) showed, using offset cultural features, that creep had been occurring south of the San Francisco Bay region along the central San Andreas fault (between 36° and 37° N latitude) for at least several decades. Subsequent monitoring along the central San Andreas fault, using alinement arrays, trilateration networks, and creepmeters (Burford and Harsh, 1980; Lisowski and Prescott, 1981; Schulz, 1989), showed a pattern of steady creep with rates approximately constant over decades for particular locations along the fault, consistent with those multidecadal rates determined by Brown and Wallace (1968). Alinement arrays tend to give the most spatially complete and accurate measurements of creep across a fault zone, because they can span the entire zone of creeping traces, which is usually narrower than 100 m (the median array length in this study is about 130 m) (Galehouse, 2002). In contrast, narrow-aperture creepmeters (a few tens of meters), although providing precise timing of creep, often considerably underestimate the amount of creep because they often fail to span the entire creeping zone. Much broader aperture geodetic networks (hundreds of meters to kilometers) tend to overestimate creep by inclusion of some elastic strain; however, they also can include some additional creep from a broader creeping zone.

After its initial documentation in 1956, creep was soon identified on the two other main faults of the San Andreas system in the San Francisco Bay region: in 1960 on the Hayward fault (Cluff and Steinbrugge, 1966) and in 1966 on the Calaveras fault (Rogers and Nason, 1971). Creep was identified on various other faults in the system in the 1970s: the Concord fault (Sharp, 1973), the Green Valley fault (Frizzell and Brown, 1976), and the Maacama fault (Harsh *et al.*, 1978). Apparent evidence of minor creep on the "Antioch fault" (Burke and Helley, 1973) turned out to be attributable to nontectonic phenomena and further study, including trenching, does not support the existence of a Holocene- or late-Pleistocene-active fault in the city of Antioch (Wills, 1992). Fault creep has also been documented on several faults in southern California (Louie *et al.*, 1985). Since its discovery in California, creep or the physically similar phenomenon of surface afterslip following earthquakes has been observed in other countries, including Turkey (Aytun, 1982), Guatemala (Bucknam *et al.*, 1978), mainland China (Allen *et al.*, 1991), Mexico (Glowacka, 1996), the Philippines (Duquesnoy *et al.*, 1994; Prioul *et al.*, 2000), Italy (Azzaro *et al.*, 2001), and Taiwan (Lee *et al.*, 2001).

The underlying causes of fault creep and the physical behavior of creeping faults have been subjects of much conjecture and study. Viscoelastic behavior dominates in creeping fault zones, so that slip tends to occur aseismically, either gradually or as events, which may last hours to days (Wesson, 1988). Creeping faults on which large ($M > 6$) earthquakes occur often exhibit postseismic surface slip that emerges slowly as afterslip (Sharp *et al.*, 1982, 1989; Lienkaemper and Prescott, 1989), but in rare cases surface coseismic slip or associated postseismic slip is absent (Harms *et al.*, 1987). The presence in the fault zone of materials that have been shown to exhibit creep in the laboratory, such as serpentinite gouges, is considered to be one possible factor promoting a creep response (Ma *et al.*, 1997). Creep may also depend on various other factors such as fault-zone geometry and fluid overpressures (Moore and Byerlee, 1991, 1992).

One focus of this article is the documentation of the along-strike variation in long-term creep rates that may be used reliably by other workers to estimate the depth of creep and thus the extent of locked zones capable of producing large earthquakes (Bürgmann *et al.*, 2000; Simpson *et al.*, 2001; Wyss, 2001; Bakun, 2003). Any particular determination of creep rate may depart from the true long-term rate of a site because of various factors, including eventfulness of creep versus gradualness, rainfall sensitivity of the site (Roeloffs, 2001), amplitude and direction of stress changes from moderate local and large regional earthquakes (Toda and Stein, 2002), width of the creeping zone, and random movements of the survey monuments (Langbein and Johnson, 1997).

We measured creep rates on San Francisco Bay region faults from September 1979 through February 2001. These data were further described and summarized in Galehouse (2001, 2002). We made over 2600 creep measurements, about one-third in the 10 years prior to the 17 October 1989, *M* 7, Loma Prieta earthquake (LPEQ) and two-thirds in the 11 years following it. Because of evidence suggesting that significant regional stress changes occurred following the LPEQ (Reasenberg and Simpson, 1992), we also include results of our monitoring before that event (Table 1). These creep measurements are continuing in the geosciences department at San Francisco State University under the direction of Karen Grove and John Caskey and at the U.S. Geological Survey (USGS) under James Lienkaemper. A detailed analysis of our results obtained on the Hayward fault was presented in Lienkaemper *et al.* (2001).

We have regular measurement sites at 29 localities on active faults, plus data from five sites that had to be abandoned (Fig. 1). Three of these sites lie outside the San Francisco Bay region, one on the San Andreas fault in the Point Arena area and two on the Maacama fault in Willits and east of Ukiah. We typically have measured sites with a history of creep about every 2 months and sites with no evidence of creep about every 3 months. In addition to our 11 regular sites on the Hayward fault (numbered sites in Fig. 1), we established 20 other sites that we began measuring annually in 1994 (shown as dots in Fig. 1 without numbers) (Lienkaemper *et al.*, 2001; Galehouse, 2002).

First we will describe the method of measurement used, then summarize our observations organized by the three dominant subsystems within the San Andreas system (Fig. 1): (1) the San Andreas fault; (2) the Hayward fault subsystem, including the Rodgers Creek and Maacama faults; and (3) the Calaveras fault subsystem, including the Northern Calaveras (north of the branch point with the Hayward fault), the Concord, and the Green Valley faults. Results from sites that monitored the San Gregorio fault system, the West Napa fault, and the former Antioch fault are presented last. Finally, we discuss these observed long-term creep rates relative to estimates of creep rate by others in the region extending from the fast-creeping, central San Andreas to the northern limit of the fault system at the Mendocino triple junction (MTJ). We present some general implications of this analysis for earthquake hazard evaluation and suggest areas where creep monitoring could be extended to help solve important unresolved issues.

Methods

The amount of right-lateral slip parallel to a fault trace is determined from changes in angles between sets of measurements taken across a fault at different times. This

Table 1

Rates of Right-Lateral Movement

Fault	WGCEP (2003) Segment	Site Number	Site	Distance from MTJ* (km)	Longitude (°)	Latitude (°)	Array Length[†] (m)	Least-Squares Average (mm/yr)	± σ	Simple Average (mm/yr)	± rw[‡]	yr	Initial Survey (dd-mmm-yy)	Final Survey (dd-mmm-yy)	Pre-Loma Prieta Earthquake[§] Least-Squares Average (mm/yr)	Pre-Loma Prieta Earthquake[§] ± σ	Pre-Loma Prieta Earthquake[§] Simple Average (mm/yr)	Pre-Loma Prieta Earthquake[§] yr
San Andreas	SAN	18	Alder Creek	131.32	−123.6895	39.0000	267	0.5	0.1	0.6	0.3	19.6	09-Jan-81	05-Aug-00	0.9	0.1	0.9	8.0
	SAN	14	Point Reyes	262.86	−122.7969	38.0441	71	0.2	0.04	0.1	0.4	15.9	04-Feb-85	13-Jan-01	0.4	0.1	0.4	4.7
	SAP	10	Duhallow Way	316.00	−122.4646	37.6443	206	−0.3	0.02	−0.2	0.3	20.8	23-Mar-80	13-Jan-01	−0.4	0.1	−0.2	9.5
	SAP	22	Roberta Drive	347.00	−122.2605	37.4171	91	0.3	0.1	0.7	0.5	11.1	04-Nov-89	26-Nov-00	—	—	0.0[ǀ]	12.7
	SAS	23	Cannon Road	429.62	−121.5851	36.8827	88	0.1	0.1	0.2	0.5	8.2	18-Nov-89	14-Feb-98	—			
	SAS	25	Mission Vineyard Rd	437.20	−121.5207	36.8351	134	10.4	0.2	11.2	0.5	10.6	21-Jul-90	25-Feb-01	—	—	14.0[ǀ]	9.6
Maacama	—	26	W. Commercial Ave	110.05	−123.3559	39.4125	126	6.5	0.1	6.6	0.5	9.3	14-Nov-91	24-Feb-01	—			
	—	31	Sanford Ranch Road	144.32	−123.1664	39.1392	263	4.4	0.2	4.5	0.5	7.8	22-May-93	10-Oct-99	—			
Rodgers Creek	RC	16	Nielson Road	228.10	−122.7083	38.4701	209	0.4	0.5	−0.9	0.6	5.4	17-Aug-80	20-Jan-86	—			
	RC	21	Roberts Road	—*	−122.6405	38.3478	199	1.6**	0.1	1.0**	0.4	14.2	20-Sep-86	26-Nov-00	—			
Hayward	HN	17	Contra Costa College	292.32	−122.3381	37.9692	107	4.9	0.1	4.6	0.3	20.4	10-Aug-80	21-Jan-01	4.7	0.3	4.2	9.0
	HN	34	Thors Bay Road	298.70	−122.2919	37.9246	120	4.3	0.1	4.5	0.4	11.3	30-Sep-89	21-Jan-01	—			
	HN	30	Florida Ave	—*	−122.2726	37.9001	74	1.4**	0.1	1.5**	0.5	8.3	12-Aug-92	12-Nov-00	—			
	HN	29	LaSalle Ave	311.81	−122.2091	37.8265	183	3.8	0.1	4.2	0.5	7.9	10-Feb-93	20-Jan-01	—			
	HS	28	Encina Way	321.30	−122.1505	37.7546	105	3.0	0.2	3.8	0.4	11.4	10-Sep-89	20-Jan-01	—			
	HS	13	Rose Street	331.16	−122.0900	37.6798	154	5.0	0.04	4.8	0.3	20.5	24-Jun-80	06-Jan-01	4.9	0.1	4.6	9.3
	HS	12	D Street	332.50	−122.0805	37.6703	136	4.4	0.03	4.5	0.3	20.5	23-Jun-80	06-Jan-01	4.9	0.1	4.9	9.3
	HS	2	Appian Way	343.59	−122.0009	37.5925	125	5.2	0.1	5.4	0.3	21.3	23-Sep-79	30-Dec-00	4.7	0.1	4.6	9.9
	HS	1	Rockett Drive	350.20	−121.9608	37.5422	180	4.8	0.1	5.0	0.3	21.3	22-Sep-79	30-Dec-00	5.5	0.1	4.5	9.9
	HS	24	Camellia Drive	354.25	−121.9343	37.5125	89	3.9	0.2	3.2	0.5	11.0	11-Feb-90	10-Feb-01	—	—	9.5[ǀ]	20.1
	HS	27	Parkmeadow Drive	354.63	−121.9317	37.5098	157	5.7	0.3	4.8	0.5	8.9	05-Apr-92	10-Feb-01	—	—	8.2[ǀ]	13.6
Green Valley	GVS	20	Red Top Road	280.40	−122.1495	38.1986	336	4.4	0.1	5.1	0.4	14.7	15-Jun-84	28-Feb-99	4.3	0.6	4.2	5.1
Concord	CON	5	Salvio Street	306.43	−122.0372	37.9758	57	2.7	0.03	2.8	0.3	21.3	30-Sep-79	11-Feb-01	2.5	0.1	3.2	9.9
	CON	3	Ashbury Drive	306.93	−122.0342	37.9720	130	3.6	0.04	3.8	0.3	21.3	28-Sep-79	11-Feb-01	3.3	0.1	3.8	9.9
Calaveras	CN	19	Corey Place	331.45	−121.9598	37.7458	111	1.6	0.1	1.7	0.3	20.2	23-Nov-80	10-Feb-01	0.2	0.1	0.3	8.6
								(3.6)	(0.1)	(3.9)	(0.5)	(8.3)						
	CN	32	Welch Creek Road	356.18	−121.8508	37.5358	164	3.6	0.5	3.5	0.8	4.0	24-Jan-97	27-Jan-01	—			
	CC	33	Coyote Ranch	415.28	−121.5242	37.0699	101	17.9	0.3	16.2	0.3	32.7	03-May-68	27-Jan-01	16.6	1.5	17.2	20.0
	CS	6	Wright Road	439.27	−121.4128	36.8699	103	9.0	0.1	9.9	0.3	21.3	21-Oct-79	25-Feb-01	12.2	0.2	12.1	9.8
	CS	4	Seventh Street	441.52	−121.4053	36.8496	90	6.4	0.1	6.6	0.3	21.4	29-Sep-79	25-Feb-01	6.4	0.2	6.8	9.9
Seal Cove	SGN	7	West Point Ave	327.39	−122.4956	37.5038	267	−0.1	0.1	−0.1	0.3	21.0	09-Nov-79	18-Nov-00	0.2	0.1	0.4	9.7
San Gregorio	SGN	8	Pescadero Road	356.45	−122.3719	37.2546	455	0.8	0.1	0.4	0.3	18.5	20-May-82	18-Nov-00	−0.8	0.6	−0.9	7.2
West Napa	—	15	Linda Vista Ave	—*	−122.3393	38.3353	131	0.1	0.1	0.0	0.3	18.5	26-Jul-80	16-Jan-99	—			
"Antioch"	—	11	Worrell Road	—*	−121.8004	37.9940	104	−0.1	0.04	−0.3	0.3	19.8	04-May-80	15-Mar-97	—			
	—	9	Deer Valley Road	—*	−121.7776	37.9605	226	1.7	0.2	1.2	0.5	7.6	21-Nov-82	01-Jul-90	—			

Site locations in Figure 1.

*MTJ: Mendocino triple junction, at downdip location where Hayward fault subsystem intersects downgoing slab. Distances given for sites located on major faults only.

**Site 21 was mistakenly located off the fault and site 30 excludes a significant fraction of the deformation zone.

[†]Lengths of array at last measurement; some arrays had multiple configurations (Galehouse, 2002).

[‡]Random walk assumption. Assumes 1σ random walk error of 1.5 $mm/yr^{0.5}$, diminishing inversely proportionate to the square root of time since the initial survey.

[§]**M** 7, 17 October 1989.

[ǀ]San Andreas fault, Burford and Harsh (1980); Hayward fault, Lienkaemper and Galehouse (1997) and Harsh and Burford (1982).

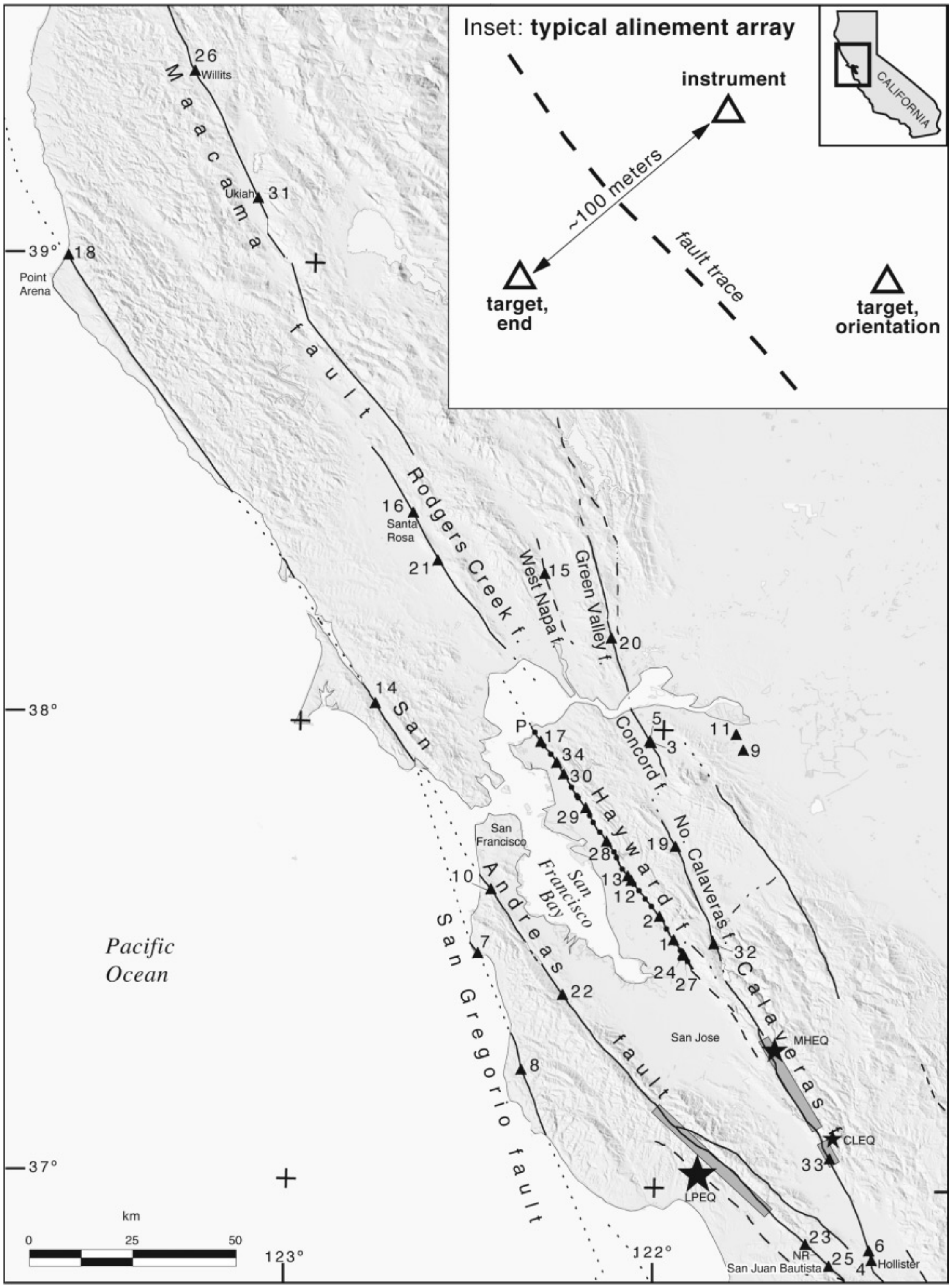

Figure 1. Holocene faults of the greater San Francisco Bay region shown as black lines. Locations of regular measurement arrays shown as triangles, annual Hayward fault arrays as dots. Numbers indicate abbreviated site names as referred to in text; for example, the full name of site 1 is "SF-1." Stars and rectangles labeled LPEQ, MHEQ, and CLEQ indicate respectively the epicenters and rupture extents of the 1989 Loma Prieta, 1984 Morgan Hill, and 1979 Coyote Lake earthquakes (Lisowski *et al.,* 1990; Oppenheimer *et al.,* 1990). Inset, typical alinement array, discussed in methods section of text. NR, Nyland Ranch, creepmeter; P, Point Pinole.

method uses a theodolite to measure the angle formed by three fixed points to the nearest tenth of a second of arc (inset, Fig. 1). The theodolite is centered and leveled over a fixed point on one side of a fault, and a target is set up over another fixed (orientation) point on the same side of the fault as the theodolite. Another target is set up over a third fixed (end) point on the opposite side of the fault. These points are emplaced such that a line from the theodolite to the end point (the fault width spanned) is as perpendicular to the local trend of the fault as is logistically possible. If not perpendicular, the measured slip needs to be corrected (increased) by dividing it by the cosine of the angle difference from the perpendicular between the fault trend and the theodolite–end point trend.

For the first 14 years of measurements, the angle was measured 12 times each measurement day using three 120° rotations of the instrument. Since then, we have simplified by measuring the angle eight times each day with one 180° rotation. This simplification in method speeds data collection and does not significantly increase the measured errors. The amount of slip between measurement days can be calculated trigonometrically using the change in average angle. The precision of the measurement method is such that we can detect with confidence any movement more than 1–2 mm between successive measurement days for most sites where length is about 100 m. Measurement error increases proportionately to length, so sites having greater length have greater error. Although the type of survey marks used varies, most are either city monuments or nails in pavement. All measurement sites span a fault width of 57–267 m, except sites 8 and 20, which span a greater width because of site considerations (Table 1). Changes in measurement lengths and all the data collected can be downloaded from Galehouse (2002). Error estimates for each survey are included with these data. The average rates of movement (Table 1) are calculated using two different methods. The least-squares average rate is determined using linear regression, and the simple average is determined by dividing the total right-lateral displacement by the total time measured.

Another estimate of error can be made assuming that the error includes a component of random walk or Brownian motion (Langbein and Johnson, 1997). The simple Gaussian error in creep rate calculated from linear regression seems implausibly low for some sites (e.g., errors < 0.1 mm/yr in Table 1). For comparison, in Table 1 we also show a more conservative random walk assumption, 1–2 mm/yr$^{0.5}$, as an estimate of error in the simple average (Langbein and Johnson, 1997). One important factor in estimating long-term creep rates, especially at sites subject to large creep events or effects of earthquakes (e.g., afterslip or triggered slip), is the relative timing of the episodes of rapid creep. The observed creep rate suddenly increases in a way that often cannot be predicted by Gaussian error estimates, but whether or not random walk estimates are a correct physical model for the timing of creep events, they do seem to encompass this aspect of uncertainty somewhat better.

Results

San Andreas Fault

All five of our measurement sites (18, 14, 10, 22, and 23) along the locked portion of the fault both northwest and southeast of the 1989 LPEQ rupture zone have remained locked (Fig. 2), showing less than 1 mm/yr of creep. At site 25, near the northwestern end of the central creeping portion of the fault just southeast of San Juan Bautista and the LPEQ rupture zone, a creepmeter showed 5 mm of right slip triggered by the LPEQ (Breckenridge and Simpson, 1997). Immediately following the LPEQ from 1990 to 1994, our measurements at site 25 show that the rate exceeded the pre–Loma Prieta rate of 14 mm/yr from 1968 to 1977 measured on an array located 300 m to the northwest (Burford and Harsh, 1980). Calculated values of static-stress changes due to the LPEQ are consistent in sign with this initially faster rate (Reasenberg and Simpson, 1992; Breckenridge and Simpson, 1997). However, creep at this site averaged about 10.4 mm/yr overall from 1990 to 2001, about 3 mm/yr slower than the rate measured on an alinement array (1968–1977) and from an offset highway pavement (1926–1978) (Burford and Harsh, 1980). The cause of the currently slower rate is likely to be the highly eventful character of the site, dominated by large creep events separated by years of quiescence (Schulz, 1989). In contrast, site 23 at Cannon Road, just north of San Juan Bautista, shows no detectable creep, but has been destroyed by a massive landslide after our last measurement on 14 February 1998. Thus, the change from a locked fault to the northwest and a creeping fault to the southeast occurs within the 4.7-km distance between site 23 and the Nyland Ranch creepmeter, where the creep rate has been ~8 mm/yr (1968–1985) (Schulz, 1989).

Hayward Fault

We measured horizontal slip at five sites (1, 2, 12, 13, and 17) along the Hayward fault for 20 years and at six more sites (24, 27, 28, 29, 30, and 34) since the LPEQ (Fig. 3). We have also been making annual measurements at 20 additional sites since 1994. The details of this collaborative research on the Hayward fault between San Francisco State University and the USGS were described at length in Lienkaemper *et al.* (2001) and Simpson *et al.* (2001) and are only briefly summarized here.

The mean, right-lateral creep rate over the northernmost 62 km of the Hayward fault is 4.6 ± 0.5 mm/yr. Although creep characteristics (steady or episodic) differ from site to site, the overall rates are quite similar, ranging from about 3.5 to 5.5 mm/yr. Detailed analyses of our results indicate that the LPEQ caused an overall slowdown in the rate of right-lateral creep along the Hayward fault, particularly near the southeastern end in Fremont, where pre-LPEQ rates had been about 9 mm/yr. The stress changes induced by the LPEQ apparently caused the creep rate on the Hayward fault in southern Fremont to decrease for several years (Galehouse, 1997; Lienkaemper *et al.*, 1997).

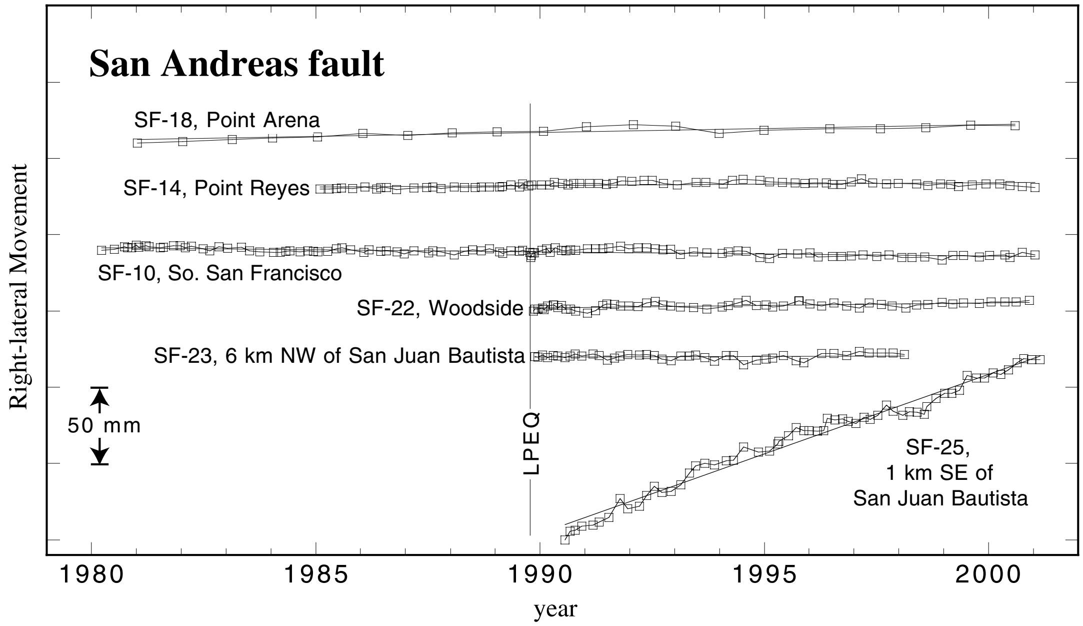

Figure 2. Right-lateral movement on arrays on the San Andreas fault. Time of LPEQ, **M** 7, Loma Prieta earthquake of 17 October 1989 is shown as vertical line. Full name of site, SF-18, referred to as "site 18" in text.

The southern end of the fault in Fremont near sites 24 and 27 showed ~9 mm/yr of right slip, about 4 mm/yr faster than the rest of the fault, for decades prior to the LPEQ (Harsh and Burford, 1982; Lienkaemper *et al.*, 1991) and probably had about 2 cm of LPEQ-triggered right slip (Lienkaemper *et al.*, 2001). For more than 6 years following the LPEQ, however, we measured very little net slip at either site (24, 27) along this portion of the fault. In fact, both sites showed a slight amount of left slip for about 4–5 years following the quake. In February 1996, however, we measured about 2 cm of right slip at both sites. This large amount of creep over a short period of time suggested a return to faster creep for this portion of the fault. However, this appears not to be the case. Site 24 has been creeping at only about 3 mm/yr since the February 1996 event, and site 27 has been creeping at about 4 mm/yr.

Reasenberg and Simpson (1992) calculated static-stress changes due to the LPEQ, which are consistent with the post-LPEQ changes in creep rate observed on the Hayward fault (Lienkaemper and Galehouse, 1997; Lienkaemper *et al.*, 1997; Lienkaemper and Galehouse, 1998).

Rodgers Creek Fault

We measured site 16 on the Rodgers Creek fault in Santa Rosa from August 1980 until we had to abandon it for logistical reasons in January 1986. During these 5 years of measurements, no significant surface slip occurred (Fig. 4), and we concluded that the Rodgers Creek fault was not creeping at this site. In September 1986, we established site 21 on a suspected trace of the Rodgers Creek fault that is now not considered to be the active trace (Hart, 1992). Although the average rate of dextral movement at site 21 was ~1 mm/yr for the 14 years of measurements, we now assume this movement was attributable to a surveying mark that had become unstable and was replaced in 1993 or to nontectonic mass movements. For future monitoring of the Rodgers Creek fault, the ongoing project has recently installed two new arrays that definitely do cross the active trace of the fault, one in Santa Rosa and another on Sonoma Mountain. Thus far no good evidence has been found to suggest that creep occurs on the Rodgers Creek fault, but south of Santa Rosa (site 16) this still remains an open question.

Maacama Fault

The Maacama fault extends 180 km from northern Sonoma County to north of Laytonville in Mendocino County and is considered to be the northwesterly continuation of the Hayward–Rodgers Creek fault trend (Galehouse *et al.*, 1992). At site 26 in Willits, the Maacama fault has been creeping right laterally at 6.5 mm/yr for the 9 years of measurements (Fig. 4). Just east of Ukiah at site 31, the fault has shown 4.4 mm/yr of right slip for the 8 years of measurements.

Calaveras Fault

Slip at two sites (4 and 6) on the southern Calaveras fault in the Hollister area has been episodic (Fig. 5), with intervals of relatively rapid right slip typically lasting 2 months or less, alternating with longer periods when little slip occurs. Creep rates before the LPEQ were 6.4 and 12.2 mm/yr, respectively. The earthquake apparently triggered up

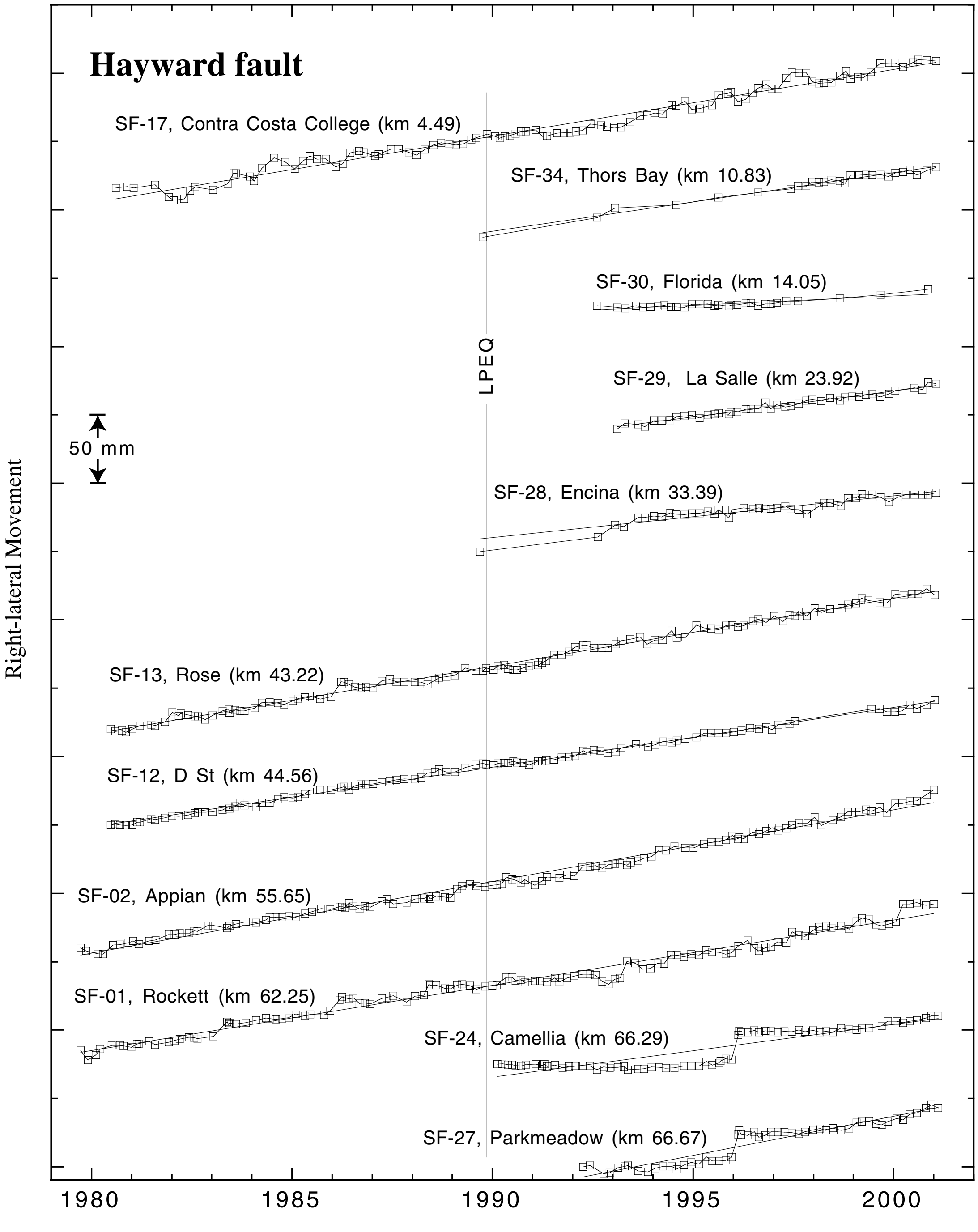

Figure 3. Right-lateral creep on regular arrays of the Hayward fault. Distances are given in kilometers southeast of Point Pinole (P, Fig. 1). Additional data are available in Lienkaemper *et al.* (2001).

to 14 mm of right slip at site 4 and up to 12 mm of right slip at site 6. After the rapid slip triggered by the LPEQ, both sites in the Hollister area returned to a slower mode of movement that persisted for several years. The static-stress changes following the LPEQ calculated by Reasenberg and Simpson (1992) are consistent with our observations of a creep slowdown on the southern Calaveras fault. The slowdown was not as pronounced at site 4, and now the pre- and post-LPEQ rates are the same (Table 1). At site 6, the fault had no net slip for nearly 4 years following the LPEQ but resumed creeping in mid-1993 at a rate a couple of millimeters per year slower than before the earthquake. A more detailed discussion of the right slip triggered by the Loma Prieta earthquake on the Calaveras fault in the Hollister area

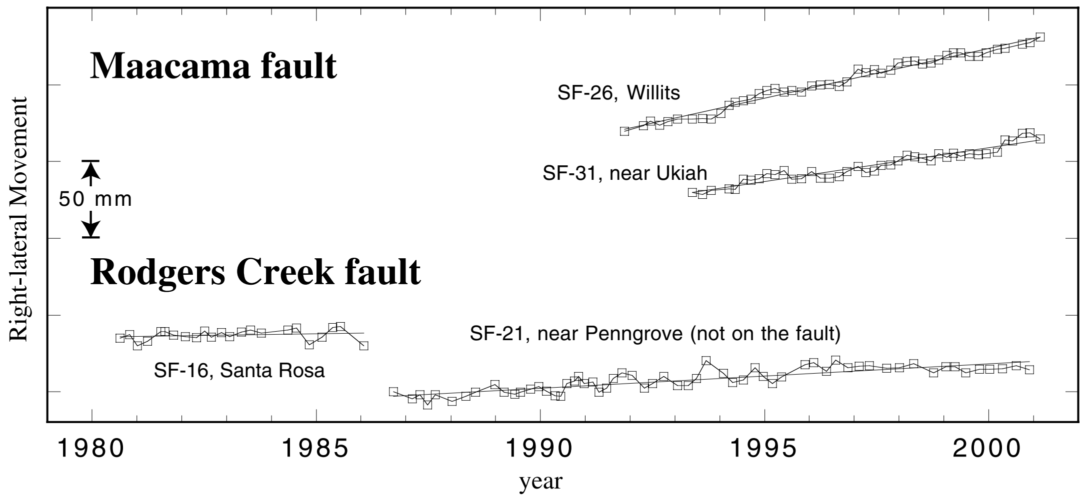

Figure 4. Right-lateral creep on faults of the Hayward fault subsystem in the North Bay: Maacama and Rodgers Creek faults.

and the effect of the Morgan Hill earthquake (MHEQ) in 1984 was given in Galehouse (1990). No immediate surface displacement had occurred at either of the Hollister area sites when they were measured the day after the MHEQ. However, within the following 2.5 months, both sites showed over a centimeter of right slip that was followed by a relatively long interval of slower slip (Fig. 5).

Site 33 on the central Calaveras fault is an old USGS alinement array site (Coyote Ranch) measured between 1968 and 1988 that showed creep at an average of about 17 mm/yr. Our new data (about 14 mm/yr for 1997–2001) added to that of the USGS still give an average rate of about 17 mm/yr for 32.7 years, the fastest creep rate in the greater San Francisco Bay region. However, it is important to note that the rate has gone through large fluctuations over these past 3 decades (Figs. 5, 6), during which three moderate to large earthquakes occurred in this area. The dominant effects of these earthquakes at site 33 are large accelerations in slip imposed by the 1979 Coyote Lake earthquake (CLEQ) and the 1984 MHEQ ruptures, even though the coseismic rupture of the latter occurred no closer than 8 km to the northwest (Fig. 1). Unfortunately, following the CLEQ, only a few observations were made at site 33. Fortunately, on a nearby short-range (~1.5-km-aperture) trilateration array, Ruby Canyon, located 2.8 km to the southeast of site 33, M. Lisowski and N. King (unpublished manuscript, 1982) observed coseismic slip (5 ± 5 mm) and 3 years of postseismic slip (142 ± 5 mm). Figure 6 shows how these geodetic results help constrain the CLEQ afterslip at site 33. Total afterslip cannot have been quite as large at site 33, but the similarity of the Ruby Canyon slip by November 1982 to the reading of site 33 immediately following the MHEQ suggests that the CLEQ afterslip was complete before the MHEQ. We show a multiple linear regression model in Figure 6 that assumes a uniform creep rate before the CLEQ acceleration and many years after the MHEQ acceleration, yielding a CLEQ step of 79.5 ± 9.7 mm, an MHEQ step of 110.1 ± 10.6 mm, and a 10.7 ± 0.6 mm/yr uniform creep rate. Introducing an LPEQ step into the model yields a similar result; thus the effect of this event has been ignored here to simplify the following discussion. For some purposes this uniform creep rate of 10.7 ± 0.6 mm/yr may be the best representation of long-term aseismic slip. However, it has been suggested by Oppenheimer *et al.* (1990) that moderate to large earthquakes such as the CLEQ and the MHEQ may be characteristic earthquakes for this part of the fault, because a similar-sized event (perhaps somewhat larger, *M* 6.5) occurred near here in 1911. What slip rate best represents the long-term average slip at this site for the purpose of forecasting larger earthquakes (e.g., $M \geq 6.7$)? For this purpose, one may reasonably account for the slip in pulses of accelerated aseismic slip following characteristic MHEQ- and CLEQ-type events by prorating them over the return period of ~73 years (1984–1911) for the MHEQ or ~68–82 years (1979–1911 or –1899 or –1897, a nonunique choice for prior event on the CLEQ segment). The rate associated with the MHEQ step at site 33 would be 1.5 mm/yr (i.e., 110 mm/73 yr) and for the CLEQ step, 1.0–1.2 mm/yr, and the net long-term rate would be 13.4 ± 0.6 mm/yr (or 13.2 ± 0.6 mm/yr if either 1897 or 1899 is used for the CLEQ prior), which is similar to the rate we have been measuring since 1997 (14 mm/yr).

Northern Calaveras Fault

In contrast to the sites in the Hollister area, site 19 in San Ramon near the northwesterly terminus of the Calaveras fault was not affected by either the MHEQ or the LPEQ (Fig. 5). It remained virtually locked throughout the first 12 years of our measurements, including 3 years following the LPEQ. However, since late 1992 at this site the fault has shown net right slip of more than 3 cm, that is, a rate of 3.6 mm/yr (Fig. 5). This suggests that the Northern Calaveras fault at this site became "unlocked" at the surface in

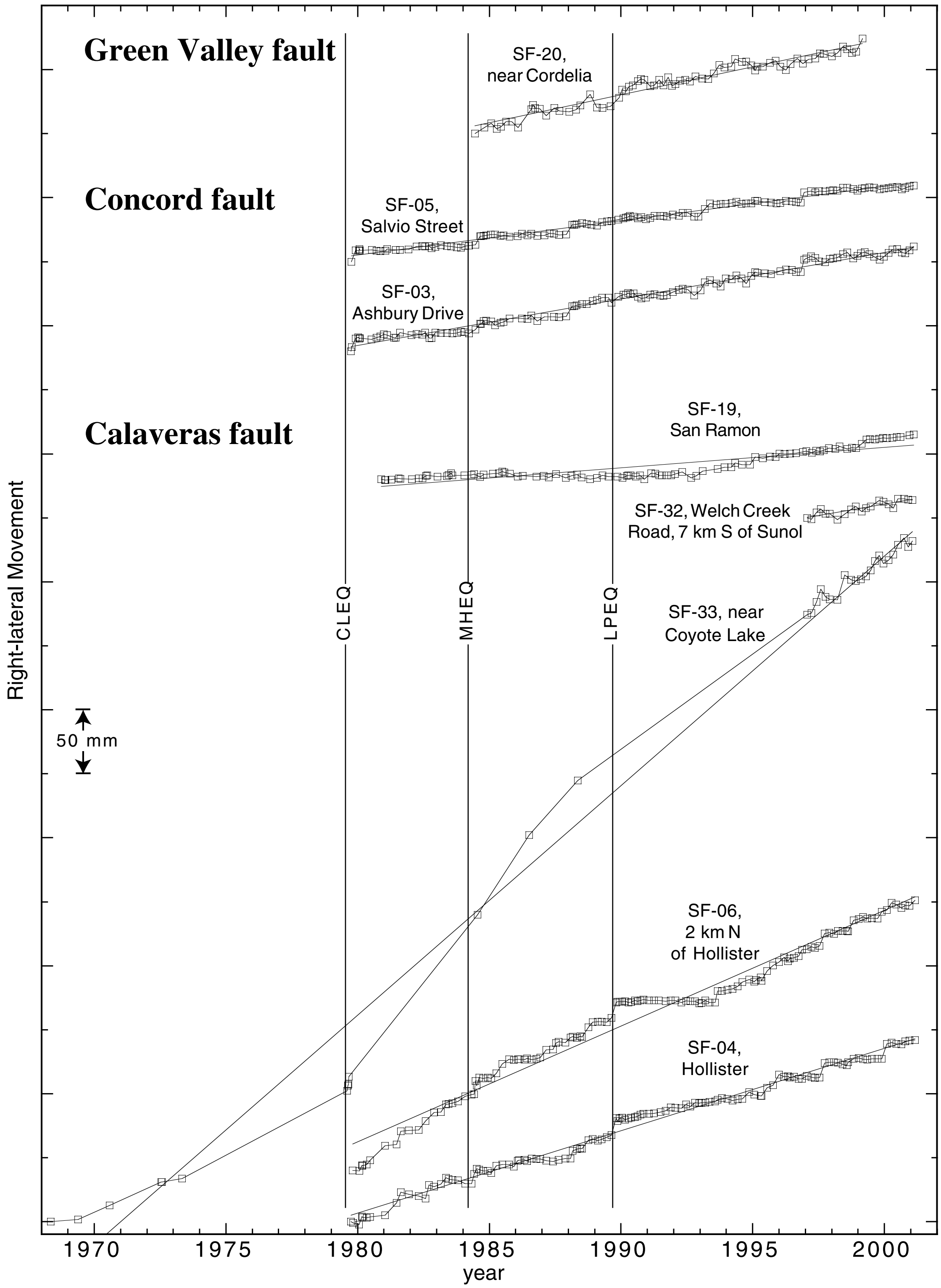

Figure 5. Right-lateral creep on faults of the Calaveras fault subsystem: Green Valley, Concord, and Calaveras faults. CLEQ, 1979 Coyote Lake earthquake; MHEQ, 1984 Morgan Hill earthquake; LPEQ, 1989 Loma Prieta earthquake.

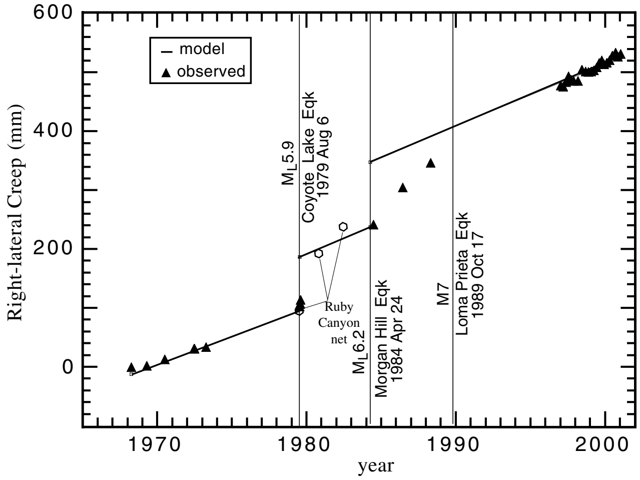

Figure 6. Right-lateral creep observed at site 33 (Coyote Ranch near Coyote Lake). Model (heavy black line) shows slip calculated by offset fit associated with the 1979 Coyote Lake and 1984 Morgan Hill earthquakes, ignoring the smaller effect of the 1989 Loma Prieta earthquake.

late 1992, a change that could have implications regarding its future seismicity.

In January 1997, we installed another array on the Northern Calaveras fault at Welch Creek Road (site 32). Although data from site 32 show large variations between measurement days, they also show a rate of 3.6 mm/yr, identical with that of site 19. Together, these two sites suggest that the Northern Calaveras fault is now creeping at about 3–4 mm/yr.

Concord–Green Valley Fault

Typical creep characteristics at sites 3 and 5 on the Concord fault in the city of Concord are intervals of relatively rapid right slip of about 7–10 mm over periods of a few months alternating with intervals of relatively slower right slip of about 1–2 mm/yr over periods of 3–5 years (Fig. 5). The latest interval of rapid right slip occurred near the end of 1996. For the 21 years of measurements, the overall average creep rate along the Concord fault in the city of Concord is about 2.5–3.5 mm/yr. It appears that the LPEQ had no effect on the creep rate of the Concord fault.

Large variations between measurement days tend to occur at site 20 on the Green Valley fault near Cordelia, possibly because of the seasonal effects of rainfall or because logistical considerations resulted in our survey line being particularly long (355 m). A series of logistical problems prevented us from obtaining reliable data from this site after 28 February 1999. Data after 28 February 1999 listed in Galehouse (2002) are suspect because they came from survey lines that were destroyed before the stability of the lines could be established. Episodes of relatively rapid slip and relatively slower slip tend to occur at different times on the Green Valley and Concord fault segments, and the rate of slip is about 1–2 mm/yr higher on the Green Valley fault (4.4 mm/yr). The episodic nature of the slip and the duration of the faster and slower intervals, however, are similar. Based on these similarities and the small right step-over between their respective fault trends, the Concord and Green Valley faults appear to be different names for the southeastern and northwestern segments of the same fault zone.

San Gregorio Fault

Virtually no creep (<1 mm/yr) has occurred at site 7 on the Seal Cove fault segment in Princeton over 21.0 years of measurements or at site 8 on the San Gregorio fault segment near Pescadero over 18.5 years (Fig. 7). Both sites, however, show large variations from one measurement day to another, probably due in part to the unusually long arrays (267 and 455 m) being measured to encompass a wide fault zone. The LPEQ does not appear to have had any noticeable effect on these two sites. They were not creeping before the LPEQ, and they still are not creeping.

West Napa Fault

No net slip occurred on the West Napa fault after 18.5 years of measurements, although there was a lot of surface "noise" at site 15 (Fig. 7). The LPEQ does not appear to have had any effect on the noncreeping West Napa fault. We had to abandon this site for logistical reasons in January 1999.

Antioch Fault

The average rate of movement had been virtually zero for 19.8 years (Fig. 7) at site 11 when it was destroyed following the 27 February 2000 measurement. The rate was about 1 mm/yr at site 9 when it had to be abandoned in July 1990. Our finding of no significant movement on the Antioch fault of Burke and Helley (1973) supports the conclusion of Wills (1992) that there is no evidence of creep on this formerly supposed active-creeping fault.

Discussion

Long-Term Creep Rates, San Andreas Fault System

Introduction. A thorough discussion of the long-term creep rates of faults in the San Francisco Bay region requires a review of earlier work, especially on the central San Andreas and the central and southern Calaveras faults, where creep is the dominant mode of surface slip and most of the earliest creep observations were made. For simplicity of analysis and discussion, we show key creep localities (Fig. 8; data shown in Table 2) on a grid approximately parallel to the Pacific plate–Sierran microplate boundary of Argus and Gordon (2001) with its origin at the MTJ. We plot creep rate versus distance along the plate boundary from the MTJ for the three principal fault subsystems that exhibit creep (Fig. 9). For purposes of this discussion we do not correct for local divergence in strike, that is, we ignore the minor component of creep normal to the plate boundary. First we

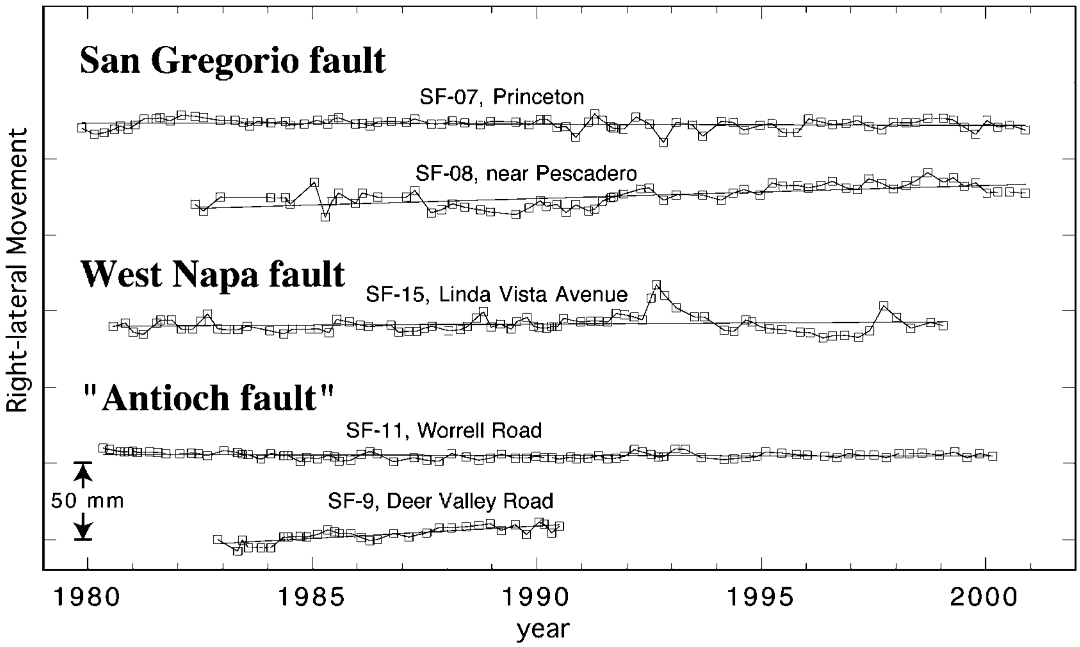

Figure 7. Right-lateral movement measurements on the San Gregorio, West Napa, and Antioch faults.

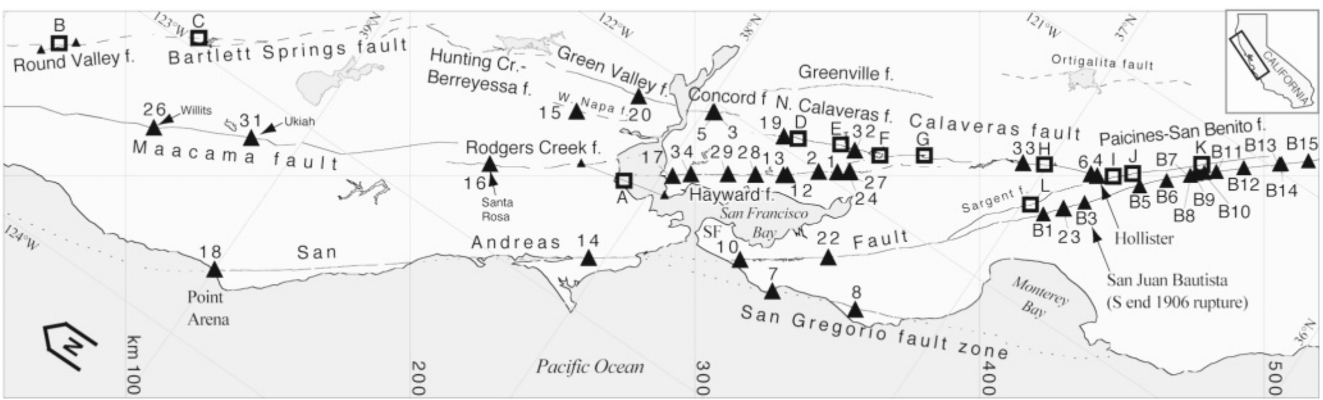

Figure 8. Map of Holocene faults within the San Andreas fault system projected approximately parallel to the Pacific–North America plate boundary near Hollister. Distances in kilometers southeast of the Mendocino triple junction (MTJ), set to 0 km where the downgoing slab intersects the Hayward fault subsystem. Alinement arrays (large triangles): numbered, this study; B1, B2, . . . , sites of Burford and Harsh (1980). Geodetic arrays or fault-crossing lines (squares): A, Sleepy–San Pablo (Lienkaemper *et al.*, 1991); B, Covelo–Poonkinney (Lisowski and Prescott, 1989); C, Slide–View (Freymueller *et al.*, 1999); D, Camp Parks (Prescott and Lisowski, 1983); E, Veras (Prescott *et al.*, 1981); F, Calaveras Reservoir (Prescott *et al.*, 1981); G, Grant Ranch (Oppenheimer *et al.*, 1990); H, San Felipe (Lisowski and Prescott, 1981 [LP81]); I, Tres Pinos (LP81); J, Thomas Road (Harsh and Pavoni, 1978); K, Pionne (LP81); L, Chase Ranch (Prescott and Burford, 1976).

summarize estimates of long-term creep rates for the three major fault subsystems that we believe are most representative of the long-term fault behavior and thus most appropriate for developing models of strain accumulation. Next we compare the creep rates for various fault segments to their long-term geologic slip rates (Fig. 10) in order to consider qualitatively whether they should be characterized as dominantly creeping, dominantly locked, or some intermediate status. Lastly we identify what we think are the most important data gaps in our present knowledge and suggest how to fill them.

Central San Andreas and Southern Calaveras Faults. The central San Andreas creeps at a maximum of about 33 mm/

Table 2
Long-Term Creep Rates along The San Andreas Fault System

Fault	Label	Site	Distance from MTJ* (km)	Creep Rate (mm/yr)	± 1σ	Type†	Period surveyed		Longitude (°)	Latitude (°)	Source
San Andreas	B01	Chamberlain	422.45	0.8	‡	A	1967	1972	− 121.6483	36.9267	Burford and Harsh, 1980
	B03	San Juan	437.09	14.0	‡	A	1968	1977	− 121.5200	36.8367	Burford and Harsh, 1980
	B05	Paicines Ranch	456.42	13.5	‡	A	1972	1977	− 121.3467	36.7200	Burford and Harsh, 1980
	B06	Lewis Ranch	465.82	14.0	‡	A	1973	1977	− 121.2717	36.6583	Burford and Harsh, 1980
	B07	Cross Willow	474.20	19.9	‡	A	1972	1977	− 121.2017	36.6050	Burford and Harsh, 1980
	B08	Willow Creek	475.95	22.7	‡	A	1972	1977	− 121.1850	36.5950	Burford and Harsh, 1980
	B09	Melendy Ranch	476.13	22.9	‡	A	1967	1978	− 121.1845	36.5933	Burford and Harsh, 1980
	B10	River Terrace	478.95	23.1	‡	A	1970	1973	− 121.1635	36.5740	Burford and Harsh, 1980
	B11	Pinnacles	483.20	23.1	‡	A	1972	1977	− 121.1350	36.5433	Burford and Harsh, 1980
	B12	Dry Lake	492.98	21.9	‡	A	1967	1974	− 121.0626	36.4762	Burford and Harsh, 1980
	B13	Eade Ranch	505.45	31.3	‡	A	1970	1976	− 120.9750	36.3883	Burford and Harsh, 1980
	B14	Smith Ranch	506.19	33.3	‡	A	1967	1971	− 120.9693	36.3833	Burford and Harsh, 1980
	B15	DeAlvarez Ranch	515.70	31.4	‡	A	1970	1977	− 120.9017	36.3167	Burford and Harsh, 1980
Maacama	26	Willits	110.05	6.5	0.1	A	1991	2001	− 123.3559	39.4125	This study
	31	Ukiah	144.32	4.4	0.2	A	1993	1999	− 123.1664	39.1392	This study
Rodgers Creek	A	Sleepy–San Pablo	276.70	1.4	1.1	T	1978	1988	− 122.4469	38.0987	Lienkaemper *et al.*, 1991
Hayward		(see Lienkaemper *et al.*, 2001)			—	—	—	—	—	—	—
Round Valley	B	Covelo–Poonkinney	76.83	8	2	T	1985	1989	− 123.2951	39.8081	Lisowski and Prescott, 1989
Bartlett Springs	C	Slide-View	125.90	8.2	2.0	G	1991	1995	− 122.9526	39.4539	Freymueller *et al.*, 1999
Green Valley	20	Red Top Rd	280.40	4.4	0.1	A	1984	1999	− 122.1495	38.1986	This study
Concord	5	Salvio Street	306.43	2.7	0.03	A	1979	2001	− 122.0372	37.9758	This study
	3	Ashbury Dr	306.93	3.6	0.04	A	1979	2001	− 122.0342	37.9720	This study
No. Calaveras	19	Corey Place	331.45	3.6	0.1	A	1993	2001	− 121.9598	37.7458	This study
	D	Camp Parks net	336.45	2.8	0.5	A	1965	1977	− 121.9359	37.7044	Lisowski and Prescott, 1989
	E	Veras net	351.39	2.9	0.3	N	1965	1976	− 121.8642	37.5810	Prescott *et al.*, 1981
	32	Welch Creek Rd	356.18	3.6	0.5	A	1997	2001	− 121.8508	37.5358	This study
	F	Calaveras Reservoir	365.30	2.2	0.5	N	1970	1979	− 121.8120	37.4578	Prescott *et al.*, 1981
Calaveras	G	Grant Ranch net	380.84	9.4	0.4	N	1977	1984	− 121.7139	37.3417	Oppenheimer *et al.*, 1990
	33	Coyote Ranch	415.28	14§	2	A	1968	2001	− 121.5242	37.0699	This study
	H	San Felipe net	422.91	13	2	N	1972	1979	− 121.4826	37.0096	Lisowski and Prescott, 1981
	6	Wright Rd	439.27	12.2	0.2	A	1979	1989	− 121.4128	36.8699	This study
				13	‡	C	1971	1983	− 121.4128	36.8699	Schulz, 1989
	4	Seventh St	441.52	6.4	0.2	A	1979	1989	− 121.4053	36.8496	This study
Calaveras (Paicines)	I	Tres Pinos	447.22	5	3	N	1975	1979	− 121.3736	36.8050	Lisowski and Prescott, 1981
	J	Thomas Rd	453.70	6.2	0.1	A	1973	1986	− 121.3233	36.7617	Harsh and Pavoni, 1978; Wilmesher and Baker, 1987
	K	Pionne net	478.20	10	3	N	1975	1979	− 121.1425	36.5932	Lisowski and Prescott, 1981
Sargent	L	Chase Ranch	417.97	2.9	0.7	A	1970	1975	− 121.6462	36.9763	Prescott and Burford, 1976

Site locations in Figure 8.
*MTJ: Mendocino triple junction, at downdip location where Hayward fault subsystem intersects downgoing slab.
†Type of data: A, alinement array; G, geodetic model; C, creepmeter; N, short-range geodetic net; T, trilateration on low-angle, fault-crossing line.
‡Source gives no estimate of error for creep rate.
§The long-term creep rate differs from the average rate in Table 1, because it accounts for effects of the CLEQ and MHEQ (see text).

yr in Bitterwater Valley (Figs. 9, 10) (Burford and Harsh, 1980). Although north of San Benito the rate drops to about 23 mm/yr, less than 3 km to the northeast the Paicines–San Benito portion of the Calaveras fault subsystem creeps at 10 ± 3 mm/yr (K, Figs. 8, 9) (Lisowski and Prescott, 1981). Thus, the net creep rate across the plate boundary remains at about 33 mm/yr. To the north, between Paicines and Hollister, creep on the San Andreas drops to 14 mm/yr, and on the Paicines (Calaveras) fault observed creep is only 5–6 mm/yr (see Fig. 8 for sources; Figs. 9, 10 for data). However, other active traces have been mapped outside of the aperture of each of these arrays on the Calaveras–Paicines fault, so these low rates may not represent the whole creeping fault zone. At the south end of the 1906 surface rupture in nearby San Juan Bautista, the rate is about 14 mm/yr (Burford and Harsh, 1980). However, the San Andreas fault creep rate drops off steeply to zero less than 7.5 km from San Juan Bautista (site 25) to the northwest at site 23.

Central Calaveras and Northern Calaveras Faults. Immediately north of Hollister, the measured Calaveras fault creep rate in recent decades ranges from about 12 to 14 mm/

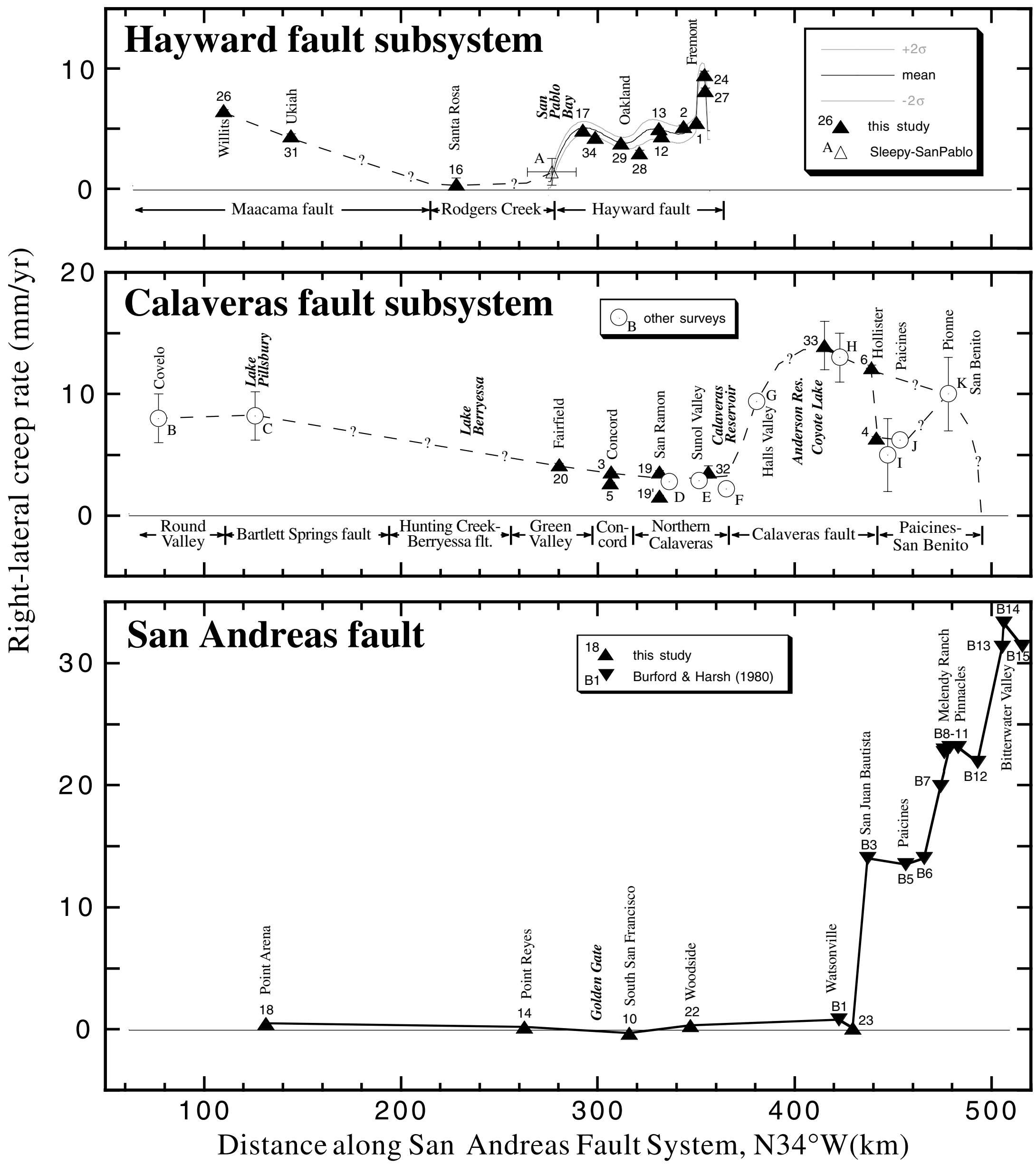

Figure 9. Long-term creep rate shown versus distance from the MTJ as described in Figure 8. Solid numbered triangles are arrays in this study; inverted solid triangles are arrays of Burford and Harsh (1980); open triangle A, span of Sleepy–San Pablo line; circles B through K, geodetic data referenced in caption of Figure 8. For the Hayward fault the mean $\pm 2\sigma$ lines show uncertainty range of best-fit polynomials that express the along-strike variation in long-term creep rate derived from the much larger data set for this fault (Lienkaemper *et al.,* 2001). Data for sites 24 and 27 reflect pre-LPEQ rates of Lienkaemper and Galehouse (1997) and Harsh and Burford (1982). Dashed lines are interpolated between available data; queries indicate areas where major gaps in the data exist. For the Paicines–San Benito section of the Calaveras subsystem, two dashed lines illustrate possible alternative interpretations of existing data.

yr, which is consistent with a 15 mm/yr (1926–1969) rate measured on an offset power line in the Hollister Valley (between H and site 6, Fig. 8) (Rogers and Nason, 1971). Between Coyote Lake and Halls Valley, the Calaveras creep rate drops from about 14 ± 2 mm/yr to 9 mm/yr. Between Halls Valley and the Calaveras Reservoir the Calaveras creep rate drops from about 9 to 2 mm/yr. At Calaveras Reservoir the Calaveras fault bends to a more northerly strike and is called the Northern Calaveras fault. At this bend the creep rate decreases to as little as 2.2 ± 0.5 mm/yr (1970–1980) (Prescott *et al.*, 1981). However, several lines of evidence suggest a creep rate of about 3–4 mm/yr on the

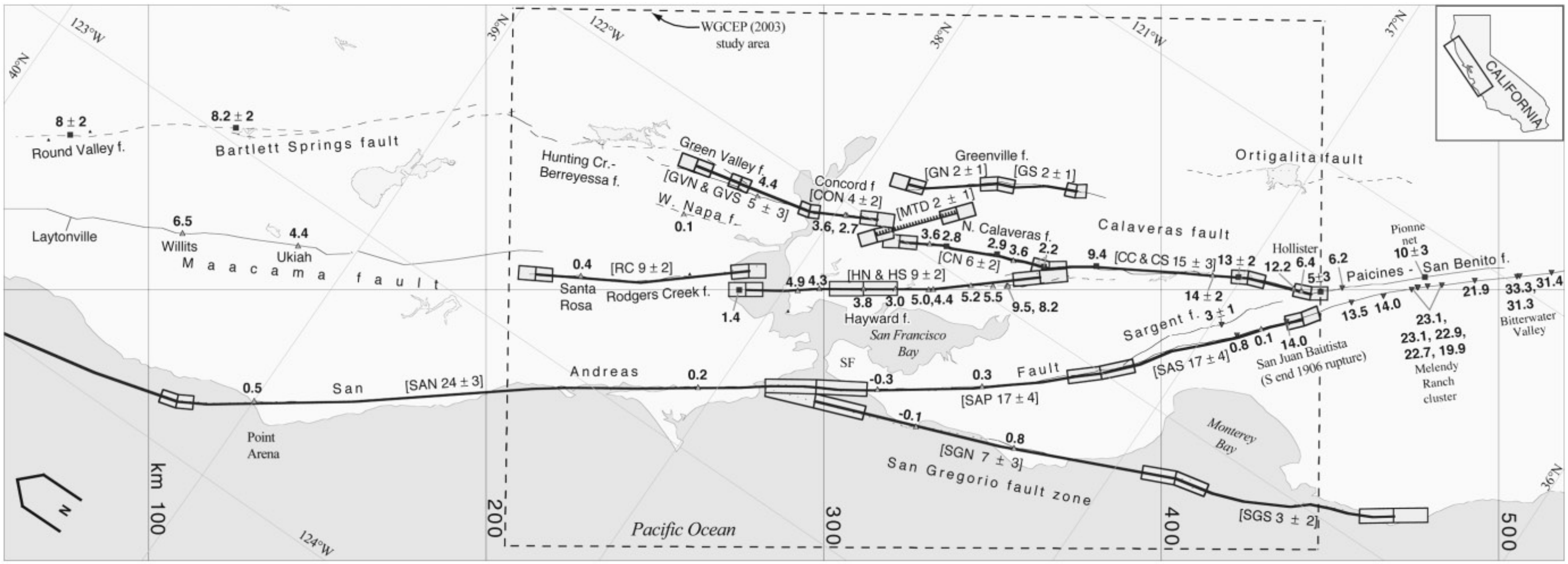

Figure 10. Long-term dextral creep rates (mm/yr) along the San Andreas fault system shown in bold type. Measured rates of movement (dextral, positive) are shown for noncreeping sites too (e.g., < 1 mm/yr). Map grid and data locations as in Figure 8. Large dashed rectangle shows limits of the WGCEP (2003) study area; fault segment name codes and long-term slip rates of WGCEP (2003) are shown in square brackets. Small rectangles show uncertainty in location of fault segment boundaries. Segment names: CN = Northern Calaveras; CC = central Calaveras; CS = southern Calaveras; CON = Concord; GN = northern Greenville; GS = southern Greenville; GVN = northern Green Valley; GVS = southern Green Valley; HN = northern Hayward; HS = southern Hayward; MTD = Mount Diablo thrust; RC = Rodgers Creek; SAN = north coast San Andreas; SAP = peninsula San Andreas; SAS = Santa Cruz Mountains San Andreas; SGN = northern San Gregorio; SGS = southern San Gregorio.

rest of the Northern Calaveras fault. Although we only have data from 1997–2001, site 32 at Welch Creek Road has a 3.6 mm/yr rate. Near Sunol Valley (E, Figs. 8, 9) rates of 3–4 mm/yr have prevailed over many decades based on offset power lines (Burford and Sharp, 1982). However, near the northern end of the Northern Calaveras at San Ramon (site 19), creep at 3.6 mm/yr did not begin until the early 1990s following 12 years of measurements showing no creep.

Hayward Fault Subsystem. Just northward of the Calaveras Reservoir the Hayward fault shows a pre-LPEQ creep rate of about 9 mm/yr in southern Fremont (Burford and Sharp, 1982; Lienkaemper *et al.*, 1991) and averages 4.6 mm/yr northward to San Pablo Bay (Lienkaemper *et al.*, 2001). We can see (Fig. 9) that in continuing northward onto the southern Rodgers Creek fault, apparently little or no creep occurs. The only constraint is about less than or equal to 1.4 $\pm$ 1.1 mm/yr fault parallel, dextral motion across a geodetic line spanning San Pablo Bay (A, Figs. 8, 9, 10). At site 16 in Santa Rosa no creep occurred during our 1980–1986 measurements. Although we have no creep information for the southern Maacama fault, creep does occur on the central Maacama, about 4.4 mm/yr near Ukiah (site 31) and 6.5 mm/yr in Willits (site 26).

Calaveras Fault Subsystem, East and North Bay. Returning to the Calaveras fault subsystem, the Northern Calaveras, with a creep rate of 3.6 mm/yr since 1992 (site 19), terminates in a right step into the Concord fault, which has similar creep rates of 2.7 (site 5) and 3.6 mm/yr (site 3). To the north, the Concord fault makes a slight bend at Suisun Bay and is called the Green Valley fault to the north. The only surveyed creep rate, 4.4 mm/yr (site 20), is consistent with the 5.4 $\pm$ 0.2 mm/yr rate from an offset power line (1922–1974) (Frizzell and Brown, 1976). Models of recent (1992–2000) Global Positioning System data suggest that the northern Green Valley fault, 15–20 km north of site 20, may not be creeping (Prescott *et al.*, 2001). If this northern part of the Green Valley fault is indeed locked, the Calaveras subsystem may be analogous to the Hayward subsystem with a locked Rodgers Creek fault and with creep resuming to the north on the Maacama fault. Although few data on creep exist for much of the northernmost Calaveras subsystem, near Lake Pillsbury and near Covelo, creep rates of about 8 mm/yr are indicated by other geodetic data (Lisowski and Prescott, 1989; Freymueller *et al.*, 1999).

Effect of Creep on Seismic Hazards

Introduction, Central San Andreas and Paicines Faults. Inferences of seismic hazards on creeping faults involve other factors in addition to variations of creep rates along fault segments. Especially important are knowledge of the long-term or geologic slip rate for each segment and the rate at which strain accumulation occurs on totally locked patches. For example, where the maximum creep rate occurs on the central San Andreas (about 33 mm/yr), the hazard is considered relatively low because this rate is virtually the same as the comparable geologic rate (33.9 $\pm$ 2.9 mm/yr) (Sieh and Jahns, 1984) at Wallace Creek in the Carrizo Plain. Still an $M \sim 6.2$ earthquake did occur near this section of the fault in 1885 (Toppozada *et al.*, 1981; Ellsworth, 1990), suggesting that some locked patches may still form here. In the 30-km reach of fault between Melendy Ranch and San Juan Bautista, the difference in net creep rate on the Paicines (Calaveras) and San Andreas faults combined suggests a deficit of about 9 mm/yr, that is, only 24 mm/yr of the 33 mm/yr expected total. Many M 5.5–6 historical earthquakes have indeed occurred in this area, but it remains uncertain if larger events might occur here, on either or both the San Andreas or Paicines (Calaveras) fault traces, which are only about 3 km apart.

Locked Fault Segments. Northward of Hollister and San Juan Bautista, the 2002 Working Group on California Earthquake Probabilities has developed, for each fault segment in the San Francisco Bay region, estimates of the fraction of its downdip rupture area (WGCEP, 2003) which can be considered locked for purposes of hazard modeling (Fig. 11) (Bakun, 2003). A subgroup within the working group considered various creep and seismicity data as well as regional geodetic models (Prescott *et al.*, 2003). The seismogenic scaling factor, R, is the fraction of the fault surface that is locked (Bakun, 2003). The downdip width of modeled rupture is multiplied by R to scale the rate at which seismic moment accumulates on a creeping fault segment. The central value estimates of locking in Figure 11 show that locking is dominant ($R \geq 0.9$) along all of the San Andreas fault in the region, except for the minor amount of creep north of San Juan Bautista. Figure 11 also shows that the working group considered the Rodgers Creek, the San Gregorio, and the Greenville faults to be mostly locked (WGCEP, 2003). Except for the unmonitored Greenville fault (which showed minor afterslip in the 1980 earthquake sequence) (Bonilla *et al.*, 1980), our monitoring evidence also indicates that these are locked segments. Because creep monitoring is not done everywhere, especially offshore, the working group gave some small weight to the possibility that some aseismic strain release may be occurring on these faults.

Seismic Potential of Partially Locked Fault Segments. In 1868 the Hayward fault had a large earthquake (M 6.8) along its southern segment (Fig. 10) (Lawson, 1908). Although the geologic slip rate (Lienkaemper and Borchardt, 1996) is well determined for the southern segment and the along-strike variation in surficial creep is known in detail (Lienkaemper *et al.*, 2001), models of the fraction locked (Simpson *et al.*, 2001) are still highly uncertain ($R = 0.6 \pm 0.2$).

The central Calaveras segment appears to have approximately the same rate of maximum creep (14 $\pm$ 2 mm/yr) as its geologic slip rate (14 $\pm$ 5 mm/yr) in the late Holocene (Kelson *et al.*, 1999) at a site located 6.2 km southeast of

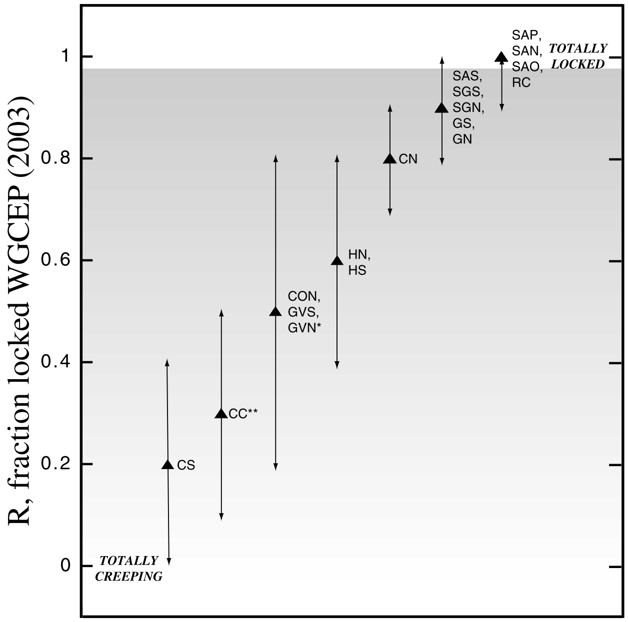

Figure 11. *R,* the fraction of each fault segment assumed to be locked in the WGCEP (2002) model, is assigned three weighted values: a central value (most likely, shown as triangles) and upper and lower bounds (arrows). $R = 1$, totally locked segment; $R = 0$, totally creeping. Segment name codes as in Figure 10. Most segments are assigned a weight of 0.6 for the central value and 0.2 for the bounds, approximating a Gaussian distribution. For highly uncertain cases, indicated by an asterisk (e.g., CON, GVS, GVN), a weight of one-third was assigned to each central value and bounds. In one case, indicated by two asterisks, evidence suggests using weights skewed toward totally creeping behavior.

site 33. Nevertheless, the *M* 6.2 MHEQ occurred along part of this segment in 1984, and one interpretation of trenching evidence by Kelson *et al.* (1999) permits **M** 7 earthquakes. The WGCEP (2003) model adopts dominantly creeping southern (CS) and central (CC) Calaveras segments ($R =$ 0.2–0.3, central values), but by assuming a broad range of possible *R* values allows that infrequently, enough strain can accumulate for an **M** 7 earthquake to occur on the central Calaveras.

The Northern Calaveras creeps at about 3–4 mm/yr and has a long-term slip rate of 6 mm/yr, a proportion much like that for the Hayward fault. However, WGCEP (2003) assumed the Northern Calaveras is more locked than the Hayward fault ($R = 0.7$–0.9 versus $R = 0.4$–0.8). An improved estimate of locking depth using all available creep data on the Northern Calaveras would probably diminish this distinction.

The Concord–Green Valley fault is assigned a broad range of possible locking ($R = 0.2$–0.8) with equal weighting to the three branches (central value and limits), because its assumed long-term slip rate (5 $\pm$ 3 mm/yr) is so uncertain. No reliable geologic slip rate is available; thus, the available creep-rate data (about 2.5–4.5 mm/yr) influence the choice of long-term slip rate. Trenching evidence supports the occurrence of large, surface-rupturing earthquakes in the last few hundred years (Baldwin and Lienkaemper, 1999). Geodetic models suggest a higher Green Valley slip rate at depth (8 $\pm$ 2 mm/yr) (Prescott *et al.*, 2001), which would increase its seismic potential.

North of the Bay Area. The Maacama fault lies outside the WGCEP (2003) study area, so its locking fraction was not estimated. Bogar (2000) documented evidence of a large recent earthquake near Ukiah, but the geologic slip rate is unknown and has been assumed to be similar to that of the Rodgers Creek and Hayward fault rate (9 $\pm$ 2 mm/yr; WGNCEP, 1996). The known creep rates of 6.5 mm/yr at Willits and 4.4 mm/yr near Ukiah suggest an intermediate level of locking similar to the Hayward fault. However, the Maacama is a 180-km-long fault zone, and its along-strike variability is not well enough sampled by our two measurement sites to characterize the entire zone.

The northernmost part of the Calaveras subsystem has not been monitored explicitly for creep, but a trilateration line crossing the Round Valley fault at a low-angle (B, Figs. 8, 9) conclusively indicated a high creep rate (8 $\pm$ 2 mm/yr), but with high uncertainty in the rate, because measurements were over only a 5-year period (Lisowski and Prescott, 1989). The Lake Pillsbury data of Freymueller *et al.* (1999) best fit a model with the Bartlett Springs fault creeping at all depths at the same rate as the Round Valley fault, 8 $\pm$ 2 mm/yr, that is, having no locking. Although long-term creep data are needed for confirmation, these preliminary geodetic observations suggest that at least parts of the Calaveras subsystem north of Lake Berryessa are predominantly creeping.

Conclusions

Previous panels that convened to forecast the probability of future large earthquakes in California neglected the effect of creep on reducing the seismic moment available for these events. The Working Group on California Earthquake Probabilities (WGCEP 1999, 2003) judged creep was “too important to ignore” (Bakun, 2003). Improved modeling of creep rate as a function of depth has begun to make good use of accurate, long-term surface creep rates like those presented here, along with regional geodetic data, to map the extent of locked patches in a fault zone. Demonstrating the lack of creep on fully locked faults is also important for seismic hazard analysis. The creep rate can abruptly change when a nearby, large earthquake changes the regional stress level. Such stress-induced changes must be accounted for in estimating long-term creep rates. Some faults, such as the Hayward, already have spatially detailed creep-rate data available adequate for modeling, whereas other important fault segments, such as the northern Green Valley, central Calaveras, Greenville, and southern Maacama, still have large critical data gaps. Work continues to fill these and other gaps, with emphasis on those faults closest to urban areas.

Acknowledgments

This project has been funded since 1979 by the U.S. Geological Survey, National Earthquake Hazards Reduction Program (the latest contract was 99-HQ-GR-0084). Special thanks go to the 23 student research assistants from San Francisco State University who have been instrumental in helping us collect the theodolite data since 1979, especially Brett Butler, Beth Brown, Carolyn Garrison, Oliver Graves, Theresa Hoyt, Forrest McFarland, Carl Schaefer, and Jim Thordson, who each worked with us on the project for more than 3 years. Reviews by R. W. Simpson, W. D. Stuart, John Langbein, and Michael Lisowski improved the clarity of the manuscript.

References

Allen, C. R., and S. W. Smith (1966). Parkfield earthquakes of June 27–29, 1966, Monterey and San Luis Obispo counties, California: preliminary report, pre-earthquake and post-earthquake surficial displacements, *Bull. Seism. Soc. Am.* **56,** 966–967.

Allen, C. R., Z. Luo, H. Qian, X. Wen, H. Zhou, and W. Huang (1991). Field study of a highly active fault zone: the Xianshuihe fault of southwestern China, *Geol. Soc. Am. Bull.* **103,** 1178–1199.

Argus, D. F., and R. G. Gordon (2001). Present tectonic motion across the Coast Ranges and San Andreas fault system in central California, *Geol. Soc. Am. Bull.* **113,** 1580–1592.

Aytun, A. (1982). Creep measurements in the Ismetpasa region of the North Anatolian fault zone, in *Multidisciplinary approach to earthquake prediction, Int. Symp. on Earthquake Prediction in the North Anatolian Fault Zone*, F. Vieweg, Wiesbaden, Germany, 279–292.

Azzaro, R., M. Mattia, and G. Puglisi (2001). Fault creep and kinematics of the eastern segment of the Pernicana fault (Mt. Etna, Italy) derived from geodetic observations and their tectonic significance, *Tectonophysics* **333,** 401–415.

Bakun, W. H. (2003). The seismogenic scaling factor, *R*, in *Earthquake probabilities in the San Francisco Bay region: 2002–2031, U.S. Geol. Surv. Open-File Rept. 03-214*, B1–B17 (http://geopubs.wr.usgs.gov/open-file/of03-214/).

Bakun, W. H., and A. G. Lindh (1985). The Parkfield, California, earthquake prediction experiment, *Science* **229,** 619–624.

Baldwin, J. N., and J. J. Lienkaemper (1999). Paleoseismic investigations along the Green Valley fault, Solano County, California, U.S. Geol. Surv., Bay Area Paleoseismological Experiment Report (contract no. 98WRCN1012).

Bernard, P. (2001). From the search of “precursors” to the research on “crustal transients,” in *The Nature of Seismic Sources and the Prediction of Earthquakes*, Elsevier, Amsterdam, 225–232.

Bogar, R. S. (2000). Paleoseismic investigation of the Maacama fault, near Talmage, California, *Master’s Thesis*, San Jose State University, California, 82 pp.

Bonilla, M. G., J. J. Lienkaemper, and J. C. Tinsley (1980). Surface faulting near Livermore, California associated with the January 1980 earthquakes, *U.S. Geol. Surv. Open-File Rept. 80–523.*

Breckenridge, K. S., and R. W. Simpson (1997). Response of U.S. Geological Survey creepmeters to the Loma Prieta earthquake, *U.S. Geol. Surv. Profess. Pap. 1550-D*, D143–D178.

Brown, R. D., Jr., and R. E. Wallace (1968). Current and historic fault movement along the San Andreas fault between Paicines and Camp Dix, California, in *Proc. of the Conf. on Geologic Problems of the San Andreas Fault System*, Stanford Univ. Pub. Geol. Sci. 11, 22–39.

Brown, R. D., Jr., J. G. Vedder, R. E. Wallace, E. F. Roth, R. W. Page, and J. P. Eaton (1967). The Parkfield–Cholame, California, earthquakes of June–August 1966: surface geologic effects, water-resources aspects, and preliminary seismic data, *U.S. Geol. Surv. Profess. Pap. 579*, 66 pp.

Bucknam, R. C., G. Plafker, and R. V. Sharp (1978). Fault movement (afterslip) following the Guatemala earthquake of February 4, 1976, *Geology* **6,** 170–173.

Burford, R. O., and P. W. Harsh (1980). Slip on the San Andreas fault in central California from alinement array surveys, *Bull. Seism. Soc. Am.* **70,** 1233–1261.

Burford, R. O., and R. V. Sharp (1982). Slip on the Hayward and Calaveras faults determined from offset powerlines, *Cal. Div. Mines Geol. Spec. Pub.* **62,** 261–269.

Bürgmann, R., D. Schmidt, R. M. Nadeau, M. d’Alessio, E. Fielding, D. Manaker, T. V. McEvilly, and M. H. Murray (2000). Earthquake potential along the northern Hayward fault, California, *Science* **289,** 1178–1182.

Burke, D. B., and E. J. Helley (1973). Map showing evidence for recent faulting in the vicinity of Antioch, Contra Costa County, California, U.S. Geol. Surv. Misc. Field Studies Map MF-533, scale 1:24,000.

Cluff, L. S., and K. V. Steinbrugge (1966). Hayward fault slippage in the Irvington–Niles districts of Fremont, California, *Bull. Seism. Soc. Am.* **56,** 257–279.

Duquesnoy, T., E. Barrier, M. Kasser, M. Aurelio, R. Gaulon, R. S. Punongbayan, C. Rangin, B. C. Bautista, E. Delacruz, M. Isada, S. Marc, J. Puertollano, A. Ramos, M. Prevot, M. Dupio, I. Eto, F. G. Sajona, D. Rigor, F. G. Delfin, and D. Layugan (1994). Detection of creep along the Philippine fault: first results of geodetic measurements on Leyte Island, central Philippines, *Geophys. Res. Lett.* **21,** 975–978.

Ellsworth, W. L. (1990). Earthquake history, 1769–1989, in *The San Andreas Fault System, California, U.S. Geol. Surv. Profess. Pap. 1515*, 153–187.

Freymueller, J. T., M. H. Murray, P. Segall, and D. Castillo (1999). Kinematics of the Pacific–North America plate boundary zone, northern California, *J. Geophys. Res.* **104,** 7419–7441.

Frizzell, V. A., and R. D. Brown (1976). Recently active breaks along the Green Valley fault, Napa and Solano counties, California, U.S. Geol. Surv. Misc. Field Invest. Map MF-743, scale 1:24,000.

Galehouse, J. S. (1990). Effect of the Loma Prieta earthquake on surface slip along the Calaveras fault in the Hollister area, *Geophys. Res. Lett.* **17,** 1219–1222.

Galehouse, J. S. (1997). Effect of the Loma Prieta earthquake on fault creep rates in the San Francisco Bay region, *U.S. Geol. Surv. Profess. Pap. 1550-D*, D193–D207.

Galehouse, J. S. (2001). Theodolite measurements of creep rates on San Francisco Bay region faults, National Earthquake Hazards Reduction Program, Annual Project Summaries 42, U.S. Geological Survey, Reston, Virginia (http://erp-web.er.usgs.gov/reports/annsum/vol42/nc/G0084.htm).

Galehouse, J. S. (2002). Data from theodolite measurements of creep rates on San Francisco Bay region faults, California: 1979–2001, *U.S. Geol. Surv. Open-File Rept. 02–225*, 94 pp. (http://geopubs.wr.usgs.gov/open-file/of02-225/).

Galehouse, J. S., J. A. Sowma-Bawcom, and C. S. Prentice (1992). The Maacama fault: preliminary creep and paleoseismic data, Mendocino County, California (abstract), *EOS* **73,** 123.

Glowacka, E. (1996). Vertical creep in the southern part of Imperial fault (Mexico) (abstract), *EOS* **77,** 516.

Harms, K. K., M. M. Clark, M. J. Rymer, M. G. Bonilla, E. L. Harp, D. G. Herd, K. R. Lajoie, J. J. Lienkaemper, S. A. Mathieson, J. A. Perkins, R. E. Wallace, J. I. Ziony, and S. N. Hoose (1987). The search for surface faulting, in *The Morgan Hill, California, Earthquake of April 24, 1984, U.S. Geol. Surv. Bull. 1639*, 61–68.

Harsh, P. W., and R. O. Burford (1982). Alinement-array measurements of fault slip in the eastern San Francisco Bay area, in *Proc. of the Conf. on Earthquake Hazards in the Eastern San Francisco Bay Area*, E. W. Hart, S. E. Hirschfield, and S. S. Schulz (Editors), Calif. Div. Mines Geol. Spec. Pub. 62, 251–260.

Harsh, P. W., and N. Pavoni (1978). Slip on the Paicines fault, *Bull. Seism. Soc. Am.* **68,** 1191–1193.

Harsh, P. W., E. H. Pampeyan, and J. M. Coakley (1978). Slip on the Willits fault (abstract), *Earthquake Notes* **49,** 22.

Hart, E. W. (1992). Recently active traces of the Rodgers Creek fault, Sonoma County, California, Calif. Div. Mines Geol Open-File Rep. 92-7, 18 pp.

Kelson, K. I., J. Tolhurst, and D. Manaker (1999). Earthquakes on the Calaveras fault: fact or fiction? The geology, seismology and paleoseismology of the Calaveras fault, in *Geologic Field Trips in Northern California*, Calif. Div. Mines Geol. Spec. Pub. 119, 160–175.

Langbein, J., and H. Johnson (1997). Correlated errors in geodetic time series: implications for time-dependent deformation, *J. Geophys. Res.* **102,** 591–604.

Lawson, A. C. (1908). The earthquake of 1868, in The California earthquake of April 18, 1906, Report of the State Earthquake Investigation Commission, Vol. 1, Carnegie Institution of Washington Publication, 434–448.

Lee, J. C., J. Angelier, H. T. Chu, J.-C. Hu, and F. S. Jeng (2001). Continuous monitoring of an active fault in a plate suture zone; a creepmeter study of the Chihshang fault, eastern Taiwan, *Tectonophysics* **333,** 219–240.

Lienkaemper, J. J., and G. Borchardt (1996). Holocene slip rate of the Hayward fault at Union City, California, *J. Geophys. Res.* **101,** 6099–6108.

Lienkaemper, J. J., and J. S. Galehouse (1997). Revised long-term creep rates on the Hayward fault, Alameda and Contra Costa counties, California, *U.S. Geol. Surv. Open-File Rept. 97–690*, 18 pp. (http://quake.usgs.gov/prepare/ncep/HF_creep/690pdf/).

Lienkaemper, J. J., and J. S. Galehouse (1998). New evidence doubles the seismic potential of the Hayward fault, *Seism. Res. Lett.* **69,** 519–523.

Lienkaemper, J. J., and W. H. Prescott (1989). Historic surface slip along the San Andreas fault near Parkfield, California, *J. Geophys. Res.* **94,** 17,647–17,670.

Lienkaemper, J. J., G. Borchardt, and M. Lisowski (1991). Historical creep rate and potential for seismic slip along the Hayward fault, California, *J. Geophys. Res.* **96,** 18,261–18,283.

Lienkaemper, J. J., J. S. Galehouse, and R. W. Simpson (1997). Creep response of the Hayward fault to stress changes caused by the Loma Prieta earthquake, *Science* **276,** 2014–2016.

Lienkaemper, J. J., J. S. Galehouse, and R. W. Simpson (2001). Long-term monitoring of creep rate along the Hayward fault and evidence for a lasting creep response to the 1989 Loma Prieta earthquake, *Geophys. Res. Lett.* **28,** 2265–2268.

Lisowski, M., and W. H. Prescott (1981). Short-range distance measurements along the San Andreas fault system in central California, 1975 to 1979, *Bull. Seism. Soc. Am.* **71,** 1607–1624.

Lisowski, M., and W. H. Prescott (1989). Strain accumulation near the Mendocino triple junction (abstract), *EOS* **70,** 1332.

Lisowski, M., W. H. Prescott, J. C. Savage, and M. J. Johnston (1990). Geodetic estimate of coseismic slip during the 1989 Loma Prieta, California, earthquake, *Geophys. Res. Lett.* **17,** 1437–1440.

Louie, J. N., C. R. Allen, D. C. Johnson, P. C. Haase, and S. N. Cohn (1985). Fault slip in southern California, *Bull. Seism. Soc. Am.* **75,** 811–833.

Ma, S., D. A. Lockner, D. E. Moore, R. Summers and J. D. Byerlee (1997). Frictional strength and velocity-dependence of serpentine gouges under hydrothermal conditions and their seismogeological implications, *Dizhen Dizhi* **19,** 171–178.

Mavko, G. M. (1982). Fault interaction near Hollister, California, *J. Geophys. Res.* **87,** 7807–7816.

Moore, D. E., and J. D. Byerlee (1991). Comparative geometry of the San Andreas fault, California, and laboratory fault zones, *Geol. Soc. Am. Bull.* **103,** 762–774.

Moore, D. E., and J. Byerlee (1992). Relationships between sliding behavior and internal geometry of laboratory fault zones and some creeping and locked strike-slip faults of California, *Tectonophysics* **211,** 305–316.

Oppenheimer, D. H., W. H. Bakun, and A. G. Lindh (1990). Slip partitioning of the Calaveras fault, California, and prospects for future earthquakes, *J. Geophys. Res.* **95,** 8483–8498.

Prescott, W. H., and R. O. Burford (1976). Slip on the Sargent fault, *Bull. Seism. Soc. Am.* **66,** 1013–1016.

Prescott, W. H., and M. Lisowski (1983). Strain accumulation along the San Andreas fault system east of San Francisco Bay, California, *Tectonophysics* **97,** 41–56.

Prescott, W. H., M. Lisowski, and J. C. Savage (1981). Geodetic measurement of crustal deformation across the San Andreas, Hayward, and Calaveras faults near San Francisco, California, *J. Geophys. Res.* **86,** 10,853–10,869.

Prescott, W., D. Manaker, R. Simpson, and W. Ellsworth (2003). *R*-factors inferred from geodetic monitoring, in *Earthquake probabilities in the San Francisco Bay region: 2002–2031, U.S. Geol. Surv. Open-File Rept. 03-214,* C1–C7 (http://geopubs.wr.usgs.gov/open-file/of03-214/).

Prescott, W. H., J. C. Savage, J. L. Svarc, and D. Manaker (2001). Deformation across the Pacific–North America plate boundary near San Francisco, California, *J. Geophys. Res.* **106,** 6673–6682.

Prioul, R., F. H. Cornet, C. Dorbath, L. Dorbath, M. Ogena, and E. Ramos (2000). An induced seismicity experiment across a creeping segment of the Philippine fault, *J. Geophys. Res.* **105,** 13,595–13,612.

Reasenberg, P. A., and R. W. Simpson (1992). Response of regional seismicity to the static stress change produced by the Loma Prieta earthquake, *Science* **255,** 1687–1690.

Roeloffs, E. A. (2001). Creep rate changes at Parkfield, California, 1966–1999: seasonal, precipitation induced, and tectonic, *J. Geophys. Res.* **106,** 16,525–16,547.

Rogers, T. H., and R. D. Nason (1971). Active displacement on the Calaveras fault zone at Hollister, California, *Bull. Seism. Soc. Am.* **61,** 399–416.

Savage, J. C., and M. Lisowski (1993). Inferred depth of creep on the Hayward fault, central California, *J. Geophys. Res.* **98,** 787–793.

Schulz, S. S. (1989). Catalog of creepmeter measurements in California from 1966 through 1988, *U.S. Geol. Surv. Open-File Rept. 89–650*, 193 pp.

Sharp, R. V. (1973). Map showing recent tectonic movement on the Concord fault, Contra Costa, and Solano counties, California, U.S. Geol. Surv. Misc. Field Invest. Map MF-505, scale 1:24,000.

Sharp, R. V., K. E. Budding, J. Boatwright, M. J. Ader, M. G. Bonilla, M. M. Clark, T. E. Fumal, K. K. Harms, J. J. Lienkaemper, D. M. Morton, B. J. O'Neill, C. L. Ostergren, D. J. Ponti, M. J. Rymer, J. L. Saxton, and J. D. Sims (1989). Surface faulting along the Superstition Hills fault zone and nearby faults associated with the earthquakes of 24 November 1987, *Bull. Seism. Soc. Am.* **79,** 252–281.

Sharp, R. V., J. J. Lienkaemper, M. G. Bonilla, D. B. Burke, B. F. Fox, D. G. Herd, D. M. Miller, D. M. Morton, D. J. Ponti, M. J. Rymer, J. C. Tinsley, J. C. Yount, J. E. Kahle, E. W. Hart, and K. E. Sieh (1982). Surface faulting in the central Imperial Valley, in *The Imperial Valley, California, Earthquake of October 15, 1979, U.S. Geol. Surv. Profess. Pap. 1254*, 119–143.

Sieh, K. E., and R. H. Jahns (1984). Holocene activity of the San Andreas fault at Wallace Creek, California, *Geol. Soc. Am. Bull.* **95,** 883–896.

Simpson, R. W., J. J. Lienkaemper, and J. S. Galehouse (2001). Variations in creep rate along the Hayward fault, California, interpreted as changes in depth of creep, *Geophys. Res. Lett.* **28,** 2269–2272.

Steinbrugge, K. V., and E. G. Zacher (1960). Creep on the San Andreas fault [California]: Fault creep and property damage, *Bull. Seism. Soc. Am.* **50,** 389–396.

Thurber, C., and R. Sessions (1998). Assessment of creep events as potential earthquake precursors: application to the creeping section of the San Andreas fault, California, *Pure Appl. Geophys.* **152,** 685–705.

Toda, S., and R. S. Stein (2002). Response of the San Andreas fault to the 1983 Coalinga–Nuñez earthquakes: an application of interaction-based probabilities for Parkfield, *J. Geophys. Res.* **107,** 10.1029/2001JB000172.

Toppozada, T. R., C. R. Real, and D. L. Parke (1981). Preparation of isoseismal maps and summaries of reported effects for pre-1900 California earthquakes, Calif. Div. Mines Geol. Open-File Rep. 81-11, 182 pp.

Wesson, R. L. (1988). Dynamics of fault creep, *J. Geophys. Res.* **93,** 8929–8951.

Wills, C. J. (1992). The elusive Antioch fault, Calif. Div. Mines Geol. Special Pub. 113, 325–331.

Wilmesher, J. F., and F. B. Baker (1987). Catalog of alinement array measurements in central and southern California from 1983 through 1986, *U.S. Geol. Surv. Open-File Rept. 87–280*, 157 pp.

Working Group on Northern California Earthquake Potential (WGNCEP) (1996). Database of potential sources for earthquakes larger than magnitude 6 in northern California, *U.S. Geol. Surv. Open-File Rept. 96–705*, 53 pp. (http://quake.wr.usgs.gov/prepare/ncep/).

Working Group on California Earthquake Probabilities (WGCEP) (1999). Earthquake probabilities in the San Francisco Bay region: 2000–2030—A summary of findings, *U.S. Geol. Surv. Open-File Rept. 99–517*, 55 pp. (http://geopubs.wr.usgs.gov/open-file/of99-517/).

Working Group on California Earthquake Probabilities (WGCEP) (2003). Earthquake probabilities in the San Francisco Bay region: 2002–2031, *U.S. Geol. Surv. Open-File Rept. 03-214* (http://geopubs.wr.usgs.gov/open-file/of03-214/).

Wyss, M. (2001). Locked and creeping patches along the Hayward fault, California, *Geophys. Res. Lett.* **28,** 3537–3540.

P.O. Box 140
Twain, California 95984
galehouse@snowcrest.net
(J.S.G.)

U.S. Geological Survey 977
Menlo Park, California 94025
jlienk@usgs.gov
(J.J.L.)

Manuscript received 6 November 2002.